ChemComm

COMMUNICATION

View Article Online
View Journal

Cite this: DOI: 10.1039/d5cc02476e

Received 1st May 2025,
Accepted 18th July 2025

DOI: 10.1039/d5cc02476e

rsc.li/chemcomm

Anion controlled selectivity in oxygen reduction catalysed by a dinuclear cobalt N,O-Schiff base complex†

Charles A. James,[a] Jessica E. Swindells,[b] Harry Ellis,[b] Richa Arjariya,[c] Samuel P. Jarvis,[c] Adam Brookfield[d] and John Fielden*[ab]

A new dinuclear cobalt complex selectively catalyses 4e$^-$ reduction of O_2 to water in methanol containing acetic acid. Its TOF of 0.031 s^{-1} and overpotential of 690 mV outperform the few previous Co N,O-chelate based catalysts for the 4e$^-$ ORR. Replacing acetic acid with NH_4PF_6 as proton source induces a complete and unprecedented switch to the H_2O_2 producing 2e$^-$ pathway. Mechanistic studies suggest a peroxo intermediate for both pathways, with acetate coordination/decoordination determining the destination of a key electron transfer.

The oxygen reduction reaction (ORR) is important to biological respiration,[1] fuel cell technology,[2] metal–air batteries[3] and aerobic oxidations.[4] The ORR in acidic media can proceed *via* two pathways; the two-electron (2e$^-$) pathway to generate hydrogen peroxide, or the four-electron (4e$^-$) pathway to water (eqn (1) and eqn (2)). As it is more exergonic and does not form the corrosive and oxidising H_2O_2, the 4e$^-$ pathway is generally preferred in the context of fuel cells. However, there is increasing interest in electrochemical synthesis of H_2O_2 *via* 2e$^-$ ORR as an alternative to the current industrial anthraquinone process,[5] and due to its importance to lithium–air batteries[3] and potential as an energy carrier.[5c,6]

$$O_2 + 4H^+ + 4e^- \rightarrow 2H_2O \quad E^\theta = 1.23\ V \qquad (1)$$

$$O_2 + 2H^+ + 2e^- \rightarrow H_2O_2 \quad E^\theta = 0.68\ V \qquad (2)$$

Molecular catalysis of the ORR in acidic organic media has been studied in detail for metalloporphyrins and phthalocyanines,[7] and Schiff base and oxime complexes,[8] but biasing the catalytic system to the 4e$^-$ rather than the 2e$^-$ pathway is challenging. Methods to increase selectivity for the 4e$^-$ pathway include: using a proton–electron transport mediator (*e.g.* hydroquinone, quinol) to facilitate O–O bond breakage,[8b,9] adding proton relays/pendant bases to facilitate protonation of bound oxygen species,[8d,10] or using Brønsted scaling relationships to disfavour H_2O_2 production.[11] Using dinuclear complexes, such as "hangman" porphyrins, to favour the 4e$^-$ pathway has also shown success.[12–16] Yet, for Co(II) salen-type complexes, which generally only catalyse the 2e$^-$ pathway, dinuclear approaches to the ORR are to our knowledge unexplored.

Herein, we show that a novel, easily accessible dinuclear Co(II) complex with a salen-like N,O chelating unit (**2**, Fig. 1) catalyses the 4e$^-$ ORR with high (>90%) selectivity, and better turnover frequency (TOF) and overpotential metrics than comparable mononuclear systems. Moreover, changing the anions in solution (from AcO$^-$ to non-coordinating PF6$^-$) enables a complete switch to the 2e$^-$ pathway, independent of the pK_a effects that control selectivity in Co(TPP) catalysts.[11] While anion/co-ligand effects are known in catalysis,[17] they are not previously reported as a way to control the pathway in the ORR.

Compound **2**, [Co_2(MeBSIP)(OAc)(H_2O)$_2$] (H_3MeBSIP = 2,2′-[(2-hydroxy-1,3-propanediyl)bis(oxy-2-benzylidineamino)]di-[4-methyl phenol], Fig. 1) was synthesised in two steps (see ESI† for full details) *via* dialdehyde precursor 2,2′-[(2-hydroxy-1,3-propanediyl)bis(oxy)] bis-benzaldehyde (**1**), which was reacted with cobalt(II) acetate and

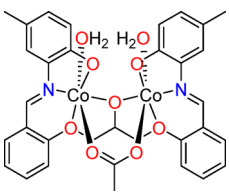

Fig. 1 Structure of the dinuclear Schiff base ORR catalyst [Co_2(MeBSIP)(OAc)(H_2O)$_2$] (**2**).

[a] School of Chemistry, University of East Anglia, Norwich Research Park, Norwich, NR4 7TJ, UK
[b] Department of Chemistry, Lancaster University, Lancaster, LA1 4YB, UK. E-mail: J.Fielden@Lancaster.ac.uk
[c] Department of Physics, Lancaster University, Lancaster, LA1 4YW, UK
[d] National Research Facility for Electron Paramagnetic Resonance Spectroscopy, University of Manchester, Oxford Road, Manchester, M13 9PL, UK

† Electronic supplementary information (ESI) available: Synthetic and other experimental details, CIF files. CCDC 2447929 and 2447930. For ESI and crystallographic data in CIF or other electronic format see DOI: https://doi.org/10.1039/d5cc02476e

2-amino-4-methylphenol to produce **2** by a templated imine condensation. Compound **2** has been characterised by ESI† mass spectrometry, CHN elemental analysis, and FTIR (Fig. S1, ESI†). CHN is consistent with the presence of two coordinated H_2O, IR indicates an imine stretch and also a bridging acetate coordination mode (ν = 1572 cm^{-1}), while MS detects a doubly charged ion at m/z = 625.066 consistent with loss of acetate and water ligands and formation of the dimer, $[Co_4(MeBSIP)_4]^{2+}$. X-ray quality crystals of **2** could not be obtained, but two structures based on the {Co_2MeBSIP} unit have been solved (Fig. 2; Table S1 and Fig. S2, S3, ESI†). Trinuclear $[Co_3(MeBSIP)(OAc)_3(MeOH)]$ (**3**) forms in the presence of excess $Co(OAc)_2$: the third Co occupies a coordination pocket defined by the two phenoxo groups, with its coordination sphere completed by acetato and methanol ligands. Defect cubane $[Co_4(MeBSIP)_2(MeOH)_2](BF_4)_2$ (**4**) was isolated by adding $NaBF_4$ to the **2** reaction mixture, and has alkoxo-bridged $[Co_2(MeBSIP)]$ units linked by formation of μ_2 and μ_3 phenolato bridges. Compounds **3** and **4** support the proposed structure of **2**, by showing {Co_2} units coordinated to MeBSIP through imine, ether and phenolate groups and a bridging alkoxo.

The strong bridging acetate IR signal of **2** supports (Fig. S3, ESI†) existence of **2** as a {Co_2} rather than {Co_4} structure, as the $[Co_4(MeBSIP)_2]^{2+}$ unit in **4** cannot accommodate bridging acetate ligands. To further support the structure of **2**, powder XPS measurements were obtained (Fig. S4, ESI†), which were consistent with a Co(II) complex containing MeBSIP and acetate ligands, moreover, distinct low temperature solid-state EPR spectra were obtained for the three compounds (Fig. S5, ESI†). Solution equilibria likely occur between the three species, but these must be slow, as assessment of the catalytic properties of **2** to **4** for O_2 reduction reveals stark differences. The three compounds were assayed for activity towards O_2 reduction in air saturated methanol, buffered by TBAOAc/HOAc, with decamethylferrocene (Fc*) as a stoichiometric reductant, with overall compositions such that [AcOH] > [Fc*] ≈ [O_2] ≫ [Catalyst]. Fc*, through the absorption of Fc^{*+} at 780 nm, also provides a spectrophotometric probe to monitor reaction progress.[13b,18] For **2**, (Fig. 3 and Fig. S6–S8, ESI†) rapid emergence of absorption at 780 nm over 10 minutes indicates that **2** catalyses oxidation of Fc* to Fc^{*+}, by reducing O_2. In the absence of **2**, the increase in [Fc*] over the same time period is *ca.* 20× smaller (Fig. S11, ESI†). Iodometric titration with NaI (Fig. 3), which detects H_2O_2 through oxidation of I^- to I_3^-, shows only a small spectral change consistent with *ca.* 10% of the O_2 being converted to H_2O_2 and thus a selectivity of around 90% for the $4e^-$ pathway to H_2O. Solubilities of **3** and **4** are poor in MeOH, but adequate concentrations (*ca.* 20 μM) could be achieved to show that **4** has almost no activity above the baseline, slow $2e^-$ reduction of O_2 to H_2O_2 by Fc*, while compound **3** shows around 1/3 of the activity of **2** (Fig. S9–S11, ESI†). This may be due to dissociation of the third Co centre, releasing active species **2**. However, aging solutions of **3** and **4** in buffer does not increase activity.

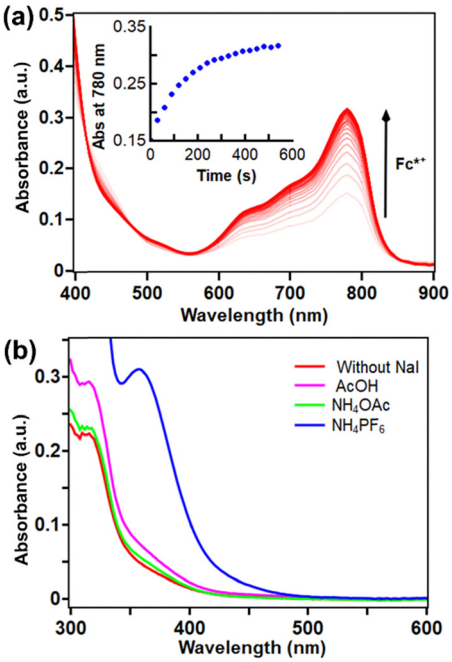

Fig. 3 (a) Evolution of the 780 nm absorption from Fc^{*+} for a solution of 20 μM **2**, 20 mM AcOH/[NBu_4][OAc] and 1 mM Fc* in air saturated MeOH. Inset: 780 nm absorbance *vs.* time. (b) Post-reaction iodometric titrations in MeCN for proton sources AcOH, (magenta) NH_4PF_6 (blue), NH_4OAc (green). 361 nm maxima are due to absorption by I_3^-.

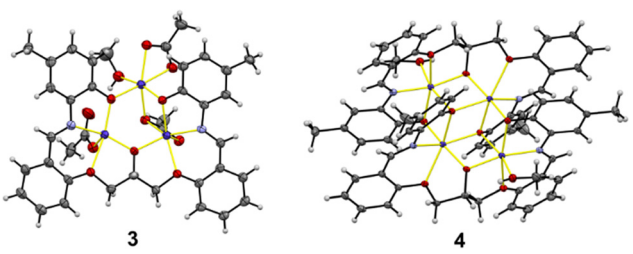

Fig. 2 X-ray crystal structures of **3**, and the $[Co_4(MeBSIP)_2(MeOH)_2]^{2+}$ complex cation in **4**. Thermal ellipsoids are at the 50% probability level, C is grey; N, blue; O, red; Co, purple, H atoms are white spheres with arbitrary radii. Coordinate bonds are shown in yellow.

A turnover frequency (TOF) for **2** for O_2 production can be estimated at 0.031 s^{-1}, with initial concentrations of [**2**] = 20 μM, [AcOH/TBAOAc] = 16 mM, and [Fc*] = 1 mM, based on the initial rate of Fc* consumption adjusted for reaction selectivity (see ESI†). As ORR catalytic rates commonly show a strong dependence on overpotential, electrochemical measurements were used to evaluate the redox potentials of **2** (Fig. 4) and further underline (Fig. S12, ESI†) that the three species remain distinct in solution. The cyclic voltammogram of **2** in MeOH (50 mM $TBAClO_4$, Fig. 4), shows two pseudo-reversible waves at $E_{1/2}$s +0.27 V (ΔE = 300 mV) and 0.83 V (ΔE = 120 mV) *vs.* $Fc^{*0/+}$. Respectively, these are assigned to the $Co^{II}Co^{II}/Co^{III}Co^{II}$ ($[2]^{0/+}$) and $Co^{III}Co^{II}/Co^{III}Co^{III}$ ($[2]^{+/2+}$) couples, the large peak separation of the $[2]^{0/+}$ process resulting from the reorganisation energy associated with a redox coupled spin crossover ($HS–Co^{II}HS–Co^{II}/LS–Co^{III}HS–Co^{II}$). The smaller ΔE for $[2]^{+/2+}$ suggests that the HS state of the second Co is stabilised as previously proposed for dinuclear cobalt complexes.[19] Adding

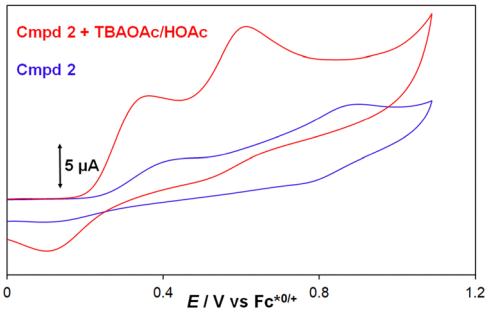

Fig. 4 Cyclic voltammetry of **2** (1 mM) before (blue) and after (red) addition of AcOH/TBAOAc (25 mM). MeOH, 50 mM $TBAClO_4$, glassy carbon electrode, 100 mV s^{-1}.

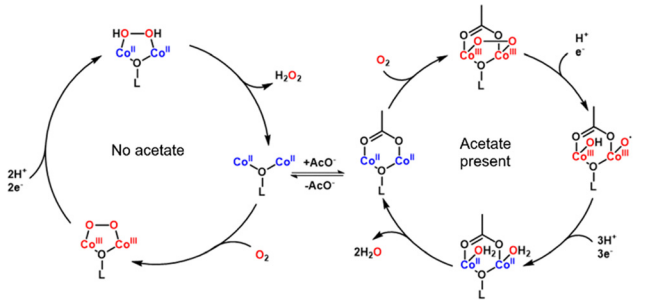

Scheme 1 Proposed mechanisms. Left: Two-electron reduction of O_2 to H_2O_2 by **2** in the absence of AcO^-. Right: Four-electron reduction of O_2 to H_2O by **2** with AcO^- present.

AcOH/TBAOAc, to recreate the conditions used in the Fc* driven ORR (Fig. 4) substantially increases the peak currents and shifts the waves to $E_{1/2}$ +0.23 (ΔE = 260 mV) and 0.56 V (ΔE = 100 mV). Increased peak currents likely result from higher conductivity due to increased total electrolyte concentration – similar behaviour is observed for $Fc^{*0/+}$ – while the negative shift in the $[\mathbf{2}]^{+/2+}$ redox potential implies an electrochemical anation reaction producing [2(OAc)] occurs on the first oxidation, the lowered charge facilitating the second process.

Like many ORR catalysts, the electrochemical response of **2** to air is too weak to distinguish an electrocatalytic wave, but the overpotential for molecular ORR catalysts (η_{eff}) can be estimated by the difference between the thermodynamic cell potential under the non-standard catalytic conditions, and the $E_{1/2}$ of the most negative catalyst redox event in the catalytic cycle: *i.e.* the $[\mathbf{2}]^{0/+}$ couple. The E_{O_2/H_2O} in 25 mM AcOH/TBAOAc in methanol can be estimated at +0.92 V *vs.* $Fc^{*0/+}$,[11] giving an overpotential for **2** of 690 mV. For this overpotential, the TOF (0.031 s^{-1}) obtained is substantially faster than can generally be projected for Fe ($<10^{-5}$)[8a] porphyrins, or Co pyridyl derivatives ($\ll 10^{-2}$) for the 4e$^-$ process.[8d,e] The literature lacks the data to enable detailed comparison with other dinuclear Co catalysts, but looking at metrics for molecular 4e$^-$ ORR catalysts in general, **2** has a high selectivity and high TOF for its overpotential, although it should be noted that mononuclear Co complexes with pendant quinols have achieved better rate and overpotential combinations.[9]

Further chemically driven ORR experiments revealed a first-order dependence on [**2**] and [Fc*], but a zero-order dependence on [O_2] between 2 and 10 mM (Fig. S17–S20, ESI†). The latter is consistent with spectroscopic and electrochemical evidence for O_2 binding by **2** (Fig. S15, S16, S26–S30, ESI†), and [O_2] being $\geq$100$\times$ greater than [**2**] (20 μM), so nearly all of the **2** is O_2 bound. The former indicate a rate-determining step involving one equivalent of **2** and one electron, likely a slow electron transfer (ET) step that facilitates breakage of the strong O–O bond. Dependence on acid concentration is more complex: increasing [AcOH] in the absence of buffer decreases rate (Fig. S21, ESI†), but increasing buffer (AcOH/TBAOAc) concentration increases rate with a near first-order dependence (Fig. S22, ESI†). At constant buffer concentration, a second-order catalytic rate equation can be constructed (eqn (3)).

$$\frac{d[\mathrm{Fc}^{*+}]}{\mathrm{dt}} = k_{\mathrm{cat}}[\mathbf{2}][\mathrm{Fc}^{*}] \quad (3)$$

Considering the rate equation, alongside electrochemical measurements and studies of related catalysts from the literature, we propose a mechanism in which water ligands dissociate from **2**, and O_2 is spontaneously and reversibly bound in an oxidative addition producing a peroxo-bridged $Co^{III}Co^{III}$ intermediate – evidenced by loss of paramagnetism in both NMR and EPR measurements (Fig. S26–S30, ESI†). Then, electron transfer (ET) to and protonation of this peroxo species results in an oxyl radical-hydroxo species which is quickly quenched by three protons and reducing equivalents to regenerate **2** (Scheme 1, right). The dependence on AcOH and AcO^- is complicated, because while protons are needed to complete the cycle, protonation of the catalyst appears to induce positive shifts in the $[\mathbf{2}]^{0/+}$ redox potential (Fig. S13, ESI†), while coordination of acetate may block substrate access.

The anion effect was further probed by changing proton source to NH_4PF_6 (pK_a in MeOH = 10.78, *vs.* 9.8 for AcOH). Remarkably, this flips the selectivity almost entirely to the 2e$^-$ pathway, with iodometric titration revealing 93% of the theoretical [H_2O_2]. To test whether this change resulted from pK_a or coordination, catalysis was performed with NH_4OAc (pK_a = 10.78) – returning the system to the 4e$^-$ pathway with 97% H_2O selectivity (Fig. 3). This result indicates that AcO^- binding is crucial to the 4e$^-$ pathway. There are two possible explanations for this: (i) without excess AcO^- in solution, decoordination of the acetate ligand destabilises the dicobalt binding site for O_2, resulting in two, connected mono-Co salen-like catalysts that operate independently: mono-Co salens favour the 2e$^-$ pathway *via* superoxo species; or (ii) the dicobalt O_2 binding site is retained, but loss of AcO^- makes the Co(III) centres more electron poor, so that electron transfer (ET) to Co and release of peroxide becomes more favourable than ET to the peroxo ligand and cleavage of the O–O bond.

Neither (i) nor (ii) can be definitively ruled out, but electrochemical, kinetic and spectroscopic evidence point towards (ii) (Scheme 1, left). Cyclic voltammetry in the presence of NH_4PF_6 (Fig. S14, ESI†) shows that the two redox processes of **2** are still

present, indicating communication between the two Co centres (*i.e.* a dinuclear binding site), but shifted to more positive potential by *ca.* 80 mV *vs.* the acetate medium. A two-site catalyst could be expected to have a lower reaction order than Fc* or the proton source, but similar rate *vs.* concentration dependencies are seen for all of these species (Fig. S23–S25, ESI†). EPR under air at room temperature, 50 K and 10 K shows no evidence of superoxo species, but the Co^{II} signals disappear in the low temperature measurements, consistent with formation of a peroxo-bridged dicobalt(III) complex. This suggests a catalytic cycle of the type shown in Scheme 1, with the rate-determining step being a final PCET step to release H_2O_2. At the estimated overpotential of 80 mV, the TOF (0.125 s^{-1}) obtained for the $2e^-$ process is *ca.* 5x higher than expected for mononuclear Co^{II} salens,[7a] which proceed *via* a Co^{III} superoxo intermediate, indicating an advantage for the dinuclear structure and consistent with a different mechanistic pathway.

In summary, we have designed and synthesised a novel dinuclear molecular catalyst with >90% selectivity for $4e^-$reduction of O_2 in acetate buffers, and >90% selectivity for the $2e^-$ pathway with non-coordinating PF_6^-. This high selectivity is combined with highly competitive TOFs (0.031/0.125 s^{-1}) relative to overpotential (690/80 mV) for both processes. Both routes appear to involve a dicobalt(III) peroxo intermediate, with coordination/decoordination of acetate modulating the proton and electron transfer properties. Future studies will establish a η_{eff} *vs.* Log(TOF) trend between similar catalysts bearing electron withdrawing and donating substituents.

We thank Mr Tom Foster and Foster Contracting Ltd for funding a PhD studentship for CAJ at UEA. SPJ and RA thank the EPSRC for support through grant EP/X026876/1. X-ray data were obtained in facilities established by EPSRC grant EP/S005854/1. JF thanks Lancaster University (LU) for funding, and JES the RSC for Undergraduate Research Bursary U24-3344520590. AB acknowledges the EPSRC for support of the UK National Research Facility for EPR (EP/W014521/1). We thank Dr Nathan Halcovitch of LU for help finalising the X-ray structures.

Conflicts of interest

There are no conflicts to declare.

Data availability

Data supporting this article are presented in the ESI† and are available at DOI:**https://doi.org/10.17635/Lancaster/researchdata/731**. Crystallographic data for **3** and **4** have been deposited at the CCDC, deposition numbers 2447929 and 2447930.†

Notes and references

1 (*a*) A. Sekretaryova, S. M. Jones and E. I. Solomon, *J. Am. Chem. Soc.*, 2019, **141**, 11304; (*b*) G. Gupta, V. Rajendran and P. Atanassov, *Electroanalysis*, 2004, **16**, 1182; (*c*) E. C. M. Tse, D. Schilter, D. L. Gray, T. B. Rauchfuss and A. A. Gewirth, *Inorg. Chem.*, 2014, **53**, 8505.
2 (*a*) M. Chisaka, *J. Mater. Chem. A*, 2024, **12**, 18636; (*b*) L. Zhang and Z. Xia, *J. Phys. Chem. C*, 2011, **115**, 11170; (*c*) Z. H. Sheng, H. L. Gao, W. J. Bao, F. Bin Wang and X. H. Xia, *J. Mater. Chem.*, 2012, **22**, 390; (*d*) H. Zhong, L. Alberto Estudillo-Wong, Y. Gao, Y. Feng and N. Alonso-Vante, *ACS Appl. Mater. Interfaces*, 2020, **12**, 21605.
3 (*a*) U. Latif, *ACS Appl. Energy Mater.*, 2025, **8**, 4838; (*b*) J. Zhang, X.-G. Zhang, J.-C. Dong, P. M. Radjenovic, D. J. Young, J.-L. Yao, Y.-X. Yuan, Z.-Q. Tian and J.-F. Li, *J. Am. Chem. Soc.*, 2021, **143**, 20049; (*c*) C. O. Laoire, S. Mukerjee, K. M. Abraham, E. J. Plichta and M. A. Hendrickson, *J. Phys. Chem. C*, 2009, **113**, 20127–20134; (*d*) X. Ren, S. S. Zhang, D. T. Tran and J. Read, *J. Mater. Chem.*, 2011, **21**, 10118.
4 (*a*) K. V. N. Esguerra, Y. Fall, L. Petitjean and J.-P. Lumb, *J. Am. Chem. Soc.*, 2014, **136**, 7662; (*b*) A. Böttcher, M. W. Grinstaff, J. A. Labinger and H. B. Gray, *J. Mol. Catal. A: Chem.*, 1996, **113**, 191; (*c*) C. Wang and J. Xiao, *Acc. Chem. Res.*, 2025, **58**, 714.
5 (*a*) J. M. Campos-Martin, G. Blanco-Brieva and J. L. G. Fierro, *Angew. Chem., Int. Ed.*, 2006, **45**, 6962; (*b*) T. Nishimi, T. Kamachi, K. Kato, T. Kato and K. Yoshizawa, *Eur. J. Org. Chem.*, 2011, 4113; (*c*) R. Zheng, Q. Meng, L. Zhang, J. Ge, C. Lui, W. Zing and M. Xiao, *Chem. – Eur. J.*, 2023, **29**, e202203180.
6 Y.-H. Wang, Z. K. Goldsmith, P. E. Schneider, C. W. Anson, J. B. Gerken, S. Ghosh, S. Hammes-Schiffer and S. S. Stahl, *J. Am. Chem. Soc.*, 2018, **140**, 10890.
7 (*a*) Y. H. Wang, B. Mondal and S. S. Stahl, *ACS Catal.*, 2020, **10**, 12031; (*b*) A. C. Brezny, S. I. Johnson, S. Raugei and J. M. Mayer, *J. Am. Chem. Soc.*, 2020, **142**, 4108; (*c*) A. Bettelheim and T. Kuwana, *Anal. Chem.*, 1979, **51**, 2257; (*d*) T. Kuwana, M. Fujihira, K. Sunakawa and T. Osa, *J. Electroanal. Chem.*, 1978, **88**, 299; (*e*) J. Zagal, M. Páez, A. A. Tanaka, J. R. dos Santos and C. A. Linkous, *J. Electroanal. Chem.*, 1992, **339**, 13; (*f*) T. Marshall-Roth, L. Liu, V. Mannava, D. M. Harraz, B. J. Cook, R. M. Bullock and Y. Surendranath, *ACS Catal.*, 2024, **14**, 18590.
8 (*a*) Y. H. Wang, M. L. Pegis, J. M. Mayer and S. S. Stahl, *J. Am. Chem. Soc.*, 2017, **139**, 16458; (*b*) C. W. Anson and S. S. Stahl, *J. Am. Chem. Soc.*, 2017, **139**, 18472; (*c*) M. A. Kamyabi, F. Soleymani-Bonoti, F. Alirezaei, R. Bikas, N. Noshiranzadeh, M. Emami, M. S. Krawczyk and T. Lis, *Appl. Organomet. Chem.*, 2019, **33**, e5214; (*d*) A. Das, A. Santra, A. Kumari, D. Ghosh and S. Paria, *J. Am. Chem. Soc.*, 2025, **147**, 6549; (*e*) A. W. Nichols, J. S. Kuehner, B. L. Huffman, P. R. Miedaner, D. A. Dickie and C. W. Machan, *Chem. Commun.*, 2021, **57**, 516.
9 S. V. Obisesan, C. Rose, B. H. Farnum and C. R. Goldsmith, *J. Am. Chem. Soc.*, 2022, **144**, 22826.
10 (*a*) S. N. Chowdhury, S. Biswas, P. Das, S. Paul and A. N. Biswas, *Inorg. Chem.*, 2020, **59**, 14012; (*b*) R. McGuire, D. K. Dogutan, T. S. Teets, J. Suntivich, Y. Shao-Horn and D. G. Nocera, *Chem. Sci.*, 2010, **1**, 411; (*c*) E. N. Cook, D. A. Dickie and C. W. Machan, *J. Am. Chem. Soc.*, 2021, **143**, 16411.
11 Y. H. Wang, P. E. Schneider, Z. K. Goldsmith, B. Mondal, S. Hammes-Schiffer and S. S. Stahl, *ACS Cent. Sci.*, 2019, **5**, 1024.
12 H. Y. Liu, M. J. Weaver, C. B. Wang and C. K. Chang, *J. Electroanal. Chem. Interfacial Electrochem.*, 1983, **145**, 439.
13 (*a*) Y. Liu, G. Zhou, Z. Zhang, H. Lei, Z. Yao, J. Li, J. Lin and R. Cao, *Chem. Sci.*, 2019, **11**, 87; (*b*) A. M. J. Devoille and J. B. Love, *Dalton Trans.*, 2011, **41**, 65.
14 G. Passard, A. M. Ullman, C. N. Brodsky and D. G. Nocera, *J. Am. Chem. Soc.*, 2016, **138**, 2925.
15 (*a*) H. Arima, M. Wada, T. Nakazono and T. Wada, *Inorg. Chem.*, 2021, **60**, 9402; (*b*) S. Fukuzumi, S. Mandal, K. Mase, K. Ohkubo, H. Park, J. Benet-Buchholz, W. Nam and A. Llobet, *J. Am. Chem. Soc.*, 2012, **134**, 9906.
16 J. Han, H. Tan, K. Guo, H. Lv, X. Peng, W. Zhang, H. Lin, U.-P. Apfel and R. Cao, *Angew. Chem., Int. Ed.*, 2024, **63**, e202409793.
17 J. Xie, Q. Zhou, C. Li, W. Wang, Y. Hou, B. Zhang and X. Wang, *Chem. Commun.*, 2014, **50**, 6520.
18 S. Fukuzumi, K. Okamoto, C. P. Gros and R. Guilard, *J. Am. Chem. Soc.*, 2004, **126**, 10441.
19 T. LeBlond and P. H. Dinolfo, *Inorg. Chem.*, 2020, **12**, 50.